Research Article

Received: 18 February 2011 Accepted: 16 April 2011 Published online in Wiley Online Library: 10 October 2011

(wileyonlinelibrary.com) DOI 10.1002/jsfa.4617

Stochastic state-space temperature regulation of biochar production. Part II: Application to manure processing via pyrolysis†

Keri B Cantrell* and Jerry H Martin II

Abstract

BACKGROUND: State-of-the-art control systems that can guarantee the pyrolytic exposure temperature are needed in the production of designer biochars. These designer biochars will have tailored characteristics that can offer improvement of specific soil properties such as water-holding capacity and cation exchange capacity.

RESULTS: A novel stochastic state-space temperature regulator was developed for the batch production of biochar that accurately matched the pyrolytic exposure temperature to a defined temperature input schedule. This system was evaluated by processing triplicate swine manure biochars at two temperatures, 350 and 700 °C. The results revealed a low coefficient of variation (CV) in their composition and near-similar ^{13}C nuclear magnetic resonance structure as well as thermal degradation patterns. When pyrolysing at 350 °C, the stochastic state-space regulator generated a biochar with lower CV in ultimate (i.e. CHNS) compositional analysis than the original feedstock.

CONCLUSION: This state-space controller had the ability to pyrolyse a feedstock and generate a consistent biochar with similar structural properties and consistent compositional characteristics.
Published 2011 by John Wiley & Sons, Ltd.

Keywords: pyrolysis; char; process control; waste treatment; waste minimization

INTRODUCTION

Thermochemical conversion technologies are becoming popular as processes for integration with current manure management strategies.[1–4] They offer numerous advantages, including both the extraction of useful energy from a livestock operation's liability and the production of value-added products.[2] Applicable technologies include gasification, hydrothermal gasification and both fast and slow pyrolysis. Slow pyrolysis of manure allows for the anaerobic production of a black carbon, a solid product often referred to as biochar. Biochar is receiving interest as a soil amendment to improve crop yields and soil quality.[3–9] Biochar behaviour in soil/plant systems has been found to vary with parent feedstock and pyrolytic temperature (see references cited in Ref. 8). Because one biochar will not be applicable as an amendment to all soils, it has been proposed that biochars should be engineered through manipulation of feedstock and the maximum pyrolytic exposure temperature to address variable soil quality issues.[5] Production of designer biochars should be conducted with pyrolytic processes that generate biochars with both high consistency and quality. This can be accomplished by employing state-of-the-art control systems that can guarantee the pyrolytic exposure temperature.

A stochastic state-space temperature regulator is one such system that controls a process based on an observed, system-descriptive state-space matrix. This state-space matrix can contain multiple temperature inputs, other process variable inputs (e.g. system pressure or mass flow rate) and derivative terms (e.g. temperature stability). State-space regulators have been discussed in previous papers related to sterilisation of food products.[10–12] State-space regulators offer better control of the sterilisation process by both avoiding undesirable degradation of nutrients and improving the quality of the final food product.[12] The application goal in food sterilisation parallels that of designer biochar production: avoid undesirable degradation during pyrolysis and generate a product with consistent structural and elemental compositions.

Details about the development of this type of regulator designed for batch, laboratory-scale production of biochar were presented in Ref. 13 that accurately matched the pyrolytic exposure temperature of biochar to a defined temperature input schedule. This regulator was developed to simultaneously control both the temperature stability of an indirect heat source and the temperature of the feedstock by employing complex variables in the description of the pyrolysis system's state-space. The present work sets out to evaluate the batch production of manure-based biochar from this system by assessing various physical and compositional characteristics of the biochar. These characteristics include elemental composition, ^{13}C nuclear magnetic resonance (NMR) spectra and thermal degradation patterns.

* *Correspondence to: Keri B Cantrell, USDA-ARS Coastal Plains Soil, Water & Plant Research Center, 2611 West Lucas Street, Florence, SC 29501-1241, USA. E-mail: keri.cantrell@ars.usda.gov*

USDA-ARS Coastal Plains Soil, Water & Plant Research Center, 2611 West Lucas Street, Florence, SC 29501-1241, USA

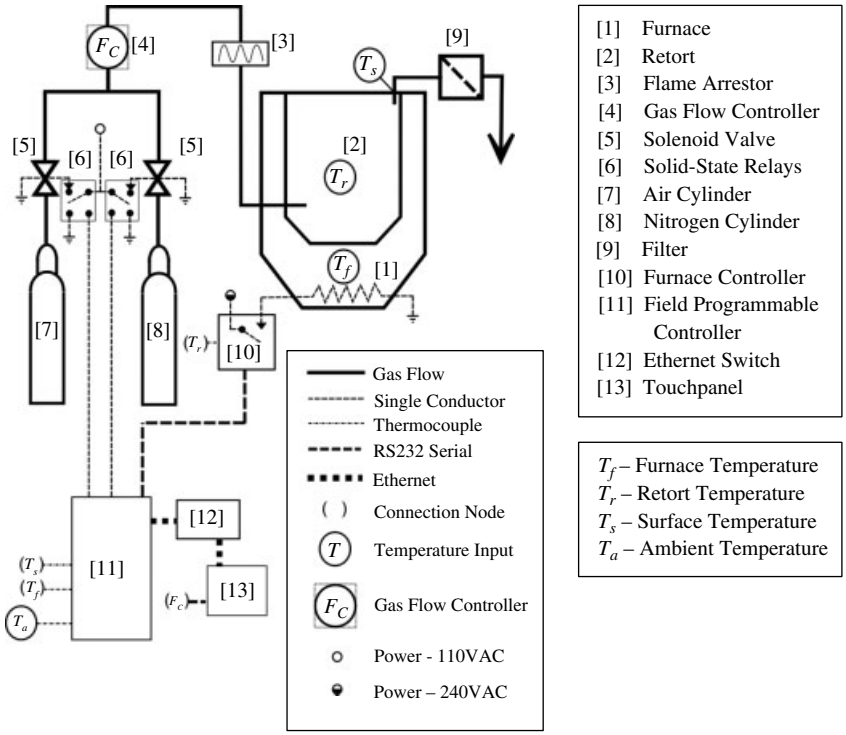

Figure 1. State-space controlled pyrolysis system design with temperature inputs indicated.

EXPERIMENTAL

Equipment selection

The pyrolysis unit was comprised of a Lindburg electric box furnace equipped with a gas-tight retort (Model 51662, Lindburg/MPH, Riverside, MI). The pyrolysis system (Fig. 1) was equipped with the following: gas cylinders containing zero-grade air (for cleaning; composed of 21.5% O_2, 78.5% N_2 and <1 ppm total hydrocarbons) and industrial-grade N_2 (for pyrolysis); two Alcon 110VAC two-way solenoid valves (ITT, White Plains, NY, USA); a 0–50 L min^{-1} gas flow controller (Model GFC37, Aalborg, Orangeburg, NY, USA); and a flame arrestor. The system was also equipped with a two-stage coalescing filter (Reading Technologies Inc., Reading, PA, USA) to remove impurities from the exhaust.

Control of this system was accomplished with a stochastic state-space controller custom programmed using Labview 2009 onto a CompactRIO Model 9073 field programmable real-time controller (National Instruments, Austin, TX, USA). The system's space-state was described by multiple temperature inputs: a thermocouple located close to the heating element on the interior of the furnace ($\boldsymbol{T}_f$); a thermocouple inside a thermal well in the top-centre of the retort ($\boldsymbol{T}_r$); a thermocouple clamped to the retort's surface ($\boldsymbol{T}_s$); a thermocouple measuring the ambient temperature ($\boldsymbol{T}_a$); and the first derivative of the furnace temperature ($\dot{\boldsymbol{T}}_f$).

Additional details on the development of this controller and the pyrolysis system can be found in Ref. 13.

Pyrolysing using stochastic state-space control

The reproducibility of biochar pyrolysed with stochastic state-space regulation was tested using a feedstock of separated swine solids. This material was collected from a polyacrylamide polymer-injected, solid-liquid separation system treating flushed manure from a 5600-head fishing swine operation in North Carolina.[14] Once collected, these separated solids underwent solar drying in a greenhouse followed by overnight drying in a 105 °C oven and then grinding using a Wiley mill with a 2 mm screen.

Triplicate pyrolytic runs were performed at two temperatures, 350 and 700 °C. For each run, between 1 and 1.5 kg of prepared material was loaded onto a stainless steel tray. This tray was placed in the retort less than 8 cm under the retort thermocouple. The sample was heated under the following temperature ramp schedule: 60 min equilibration hold at 200 °C; ramp to desired pyrolytic temperature within 60 min (2.5 °C min^{-1} for 350 °C runs; 8.33 °C min^{-1} for 700 °C runs); 120 min equilibration hold at desired temperature; 4.25 °C min^{-1} cool down to 100 °C. During the 200 °C hold, the retort was purged using an industrial-grade N_2 gas flow at 15 L min^{-1}; the N_2 flow for the remaining operation was set to 1 L min^{-1} (equivalent to 0.6 and 0.04 retort chamber exchanges per minute respectively) to maintain anoxic conditions. After charring, the samples were allowed to cool and were then removed from the retort and homogeneously subsampled for analyses.

Feedstock and biochar analyses

Both raw feedstock and biochar subsamples underwent analyses to determine their composition, thermal and pyrolytic degradation properties and distribution of carbon among structural groups. The composition was determined by ultimate, proximate, higher heating value (HHV), nutrient, pH and electrical conductivity (EC) analyses. The ultimate analysis was done by Hazen Research, Inc. (Golden, CO, USA) following ASTM D 3176 (CHNS and O by difference).[15] For the proximate analysis the ash content at 600 °C was determined by Hazen Research, Inc., the volatile matter was determined using a thermogravimetric analyser (TGA/DSC1, Mettler Toledo International Inc., Columbus, OH, USA) following the method of Cantrell *et al.*,[16] and the fixed carbon content was determined (following ASTM D 3172) as the difference from 100% of volatile matter and ash.[15] The HHV or energy content was

determined using an isoperibol calorimeter (AC500, Leco Corp., St Joseph, MI, USA) following ASTM D 5865 and corrected for N and S content before conversion to a dry basis ('db') as well as a dry ash-free basis ('daf').[15] Elemental analyses of Al, As, B, Cd, Ca, Cr, Cu, Fe, Mg, Mn, Mo, Ni, P, K, Na, S and Zn were performed by the Agricultural Service Laboratory at Clemson University (Clemson, SC, USA) using wet acid digestion (conc. HNO_3 + 30% H_2O_2) with elements quantified by inductive coupled plasma (ICP). The pH and EC of the feedstock and biochars were measured in triplicate in deionised water at 10 g/L after shaking at 100 rpm for 2 h. One-way analysis of variance (ANOVA) was performed on selected characteristics using SAS Version 9.2 (SAS Institute Inc., Cary, NC, USA).

The combustion and pyrolytic degradation characteristics of both the feedstock and biochars were analysed using the TGA/DSC1 that operated under a three-point In, Al and Au temperature calibration. All samples were placed in 70 µL AlO_3 crucibles and dried as described by Cantrell *et al.*[16] to allow assessment on a dry weight basis. The samples were heated under a constant 10 °C min^{-1} temperature ramp from 40 to 950 °C, and the mass loss (thermogravimetry, TG) curves of these samples were recorded while being either pyrolysed under a 60 mL min^{-1} flow of ultrahigh-purity N_2 or oxidised under a 60 mL min^{-1} flow of zero-grade air.

The distribution of carbon among the biochar's structural groups and one raw feedstock sample was determined using solid-state cross-polarisation magic angle-spinning total sideband suppression ^{13}C NMR spectroscopy; spectral patterns were obtained using a Bruker Avance DSX300 spectrometer (Rheinstetten, Germany) operated at a ^{13}C frequency of 75.5 MHz. Additional technical parameters to acquire the spectra have been described previously.[17] The chemical shift region spectral assignments were as follows: 0–50 ppm, aliphatic-C; 50–61 ppm, methoxy-C; 61–96 ppm, alcoholic-C; 96–109 ppm, O-alkyl-C; 109–145 ppm, aromatic-C; 145–163 ppm, phenolic-C; 163–190 ppm, carboxylic-C; 190–220 ppm, carbonyl-C.[17]

Recovery yields

For each run, four recovery yields were determined: C, ash, biochar and biochar energy. The biochar recovery was the percentage ratio of biochar mass to feedstock mass. The C recovery was calculated as the percentage ratio of the total C in the biochar mass to the total C in the feedstock mass (i.e. 100 × (mass × C content of biochar)/(mass × C content of feedstock)). The ash and biochar energy recoveries were calculated similarly.

RESULTS AND DISCUSSION

Biochar recovery yields and energy characteristics

As expected, increasing the pyrolytic temperature decreased the biochar recovery (Table 1). At 350 °C the biochar yield recovery was on average 62.3%. As the pyrolytic temperature increased to 700 °C, the yield declined to 36.4%. Carbon recoveries (ratio of biochar C to feedstock C) for the low and high temperatures tested were 67.7 and 33.8% respectively. Following a similar pattern was the biochar energy recovery, with 67.9% of the energy in the feedstock being recovered in the biochar at 350 °C but only 28.3% at 700 °C. Ash recoveries ranged from 97.0% (350 °C) to 92.1% (700 °C).

Pyrolysing raw swine solids was found to have opposite effects on pH and EC. The pH of the biochars increased slightly from that of the raw feedstock, from 7.97 to a maximum of 8.20 (700 °C biochar).

Table 1. Proximate analysis, HHV, pH, EC and recoveries (mean and CV) of separated swine solids and biochars at 350 and 700 °C

	Swine solids		350 °C biochar		700 °C biochar	
Parameter	Mean	CV	Mean	CV	Mean	CV
pH	7.97a	0.3	8.16b	0.6	8.20b	0.7
EC (µS m^{-2})	846a	4	208b	4	174b	2
HHV (MJ kg_{db}^{-1})	19.4a	0.8	21.1b	2.0	15.1c	2.2
HHV (MJ kg_{daf}^{-1})	24.5a	1.1	31.3b	0.9	32.0b	2.5
Proximate analysis (g kg_{db}^{-1})[a]						
Volatile matter	736	0.4	498	1.1	134	2.1
Fixed C	55	1.9	177	6.7	337	1.6
Ash	209	1.8	325	2.6	529	0.9
Recoveries (%)						
Biochar energy[b]	–		67.9	3.1	28.3	1.6
Biochar[c]	–		62.3	1.2	36.4	0.9
Ash[d]	–		97.0	2.1	92.1	0.6
C[e]	–		67.7	2.7	33.8	0.7

Means within a row followed by different letters are significantly different by one-way ANOVA at $\alpha = 0.05$.
[a] ASTM D 3172 with ash determined at 600 °C and fixed C calculated as 100 − volatile matter − ash.
[b] Percentage ratio of total energy of biochar to total energy of feedstock (mass × HHV of biochar/mass × HHV of feedstock).
[c] Percentage ratio of biochar mass to feedstock mass.
[d] Percentage ratio of total ash in biochar mass to total ash in feedstock mass.
[e] Percentage ratio of total C in biochar mass to total C in feedstock mass.

However, one-way ANOVA indicated no significant difference in pH between the 350 and 700 °C biochars. This behaviour was not observed at the same processing temperatures for other poultry litter or pecan shell biochars, where there were marked increases in pH with additional increases in pyrolytic temperature.[5] The EC of the biochars responded inversely to an increase in temperature, with the raw feedstock having an observed EC of 846 µS m^{-2} that decreased to 174 µS m^{-2} (700 °C biochar).

Compared with the raw feedstock, increasing the pyrolytic temperature slightly increased the HHV of the biochar when processed at 350 °C, from 19.4 to 21.1 MJ kg_{db}^{-1}. A further pyrolytic temperature increase caused a decrease in the biochar energy content by 31% to 15.1 MJ kg_{db}^{-1}. This range of temperatures and resulting HHV for swine solids was within the range for swine solid biochar produced by a pilot commercial system that generated a biochar at 620 °C yielding 18.3 MJ kg_{db}^{-1}.[18] With respect to the HHV on a dry ash-free basis, pyrolysis increased the energy content of the swine solids, suggesting changes in the carbon structure that were more energy-dense.

With pyrolysis being a devolatilisation process, the results show that more volatile matter was removed with increasing temperature. Thus there was an associated one- to threefold increase in the ash content. In addition to ash increases, the fixed C content increased to three to six times the original. The fixed C content in the 700 °C biochar (337 g kg_{db}^{-1}) was less than that previously reported for swine char processed at 620 °C (412 g kg_{db}^{-1}).[18]

Biochar elemental and structural characteristics

For the pyrolysis system tested, the stochastic state-space controller processed a feedstock with a heterogeneous composition

Table 2. Ultimate and elemental analyses (mean and CV) of separated swine solids and biochars at 350 and 700 °C (data sorted into macroelement and microelement pools)

	Swine solids		350 °C biochar		700 °C biochar	
Element	Mean	CV	Mean	CV	Mean	CV
Ultimate analysis (g kg_{db}^{-1})[a]						
C	474.2	0.2	515.1	1.7	440.6	0.3
H	60.1	3.7	49.1	2.0	7.4	15.1
N	41.1	3.9	35.4	0.4	26.1	2.5
S	9.4	2.7	8.0	1.4	8.5	3.1
O[b]	206	4.9	67.4	2.3	0.0	–
Macroelements (g kg_{db}^{-1})						
Al	0.786	5.2	1.17	1.9	2.14	0.9
Ca	23.9	4.5	39.1	1.2	61.5	5.2
Cu	0.918	2.0	1.54	1.4	2.49	4.5
Fe	3.15	13.2	4.84	0.8	7.48	6.1
K	10.9	2.5	17.8	1.6	25.7	9.9
Mg	15.0	3.1	24.4	1.5	36.9	7.2
Mn	0.907	3.4	1.45	0.5	2.27	5.0
Na	3.62	4.1	5.98	2.5	9.35	6.8
P	24.7	3.2	38.9	1.2	59.0	4.6
S[c]	7.86	3.3	7.48	0.4	8.09	4.9
Zn	1.96	3.3	3.18	1.4	5.00	3.5
Microelements (mg kg_{db}^{-1})						
As	0.72	18.7	0.90	11.1	1.64	21.1
B	34.8	3.5	55.7	1.8	89.0	2.0
Cd	0.27	21.9	0.57	10.2	0.28	8.8
Cr	14.9	2.7	24.8	0.8	37.3	6.6
Mo	10.9	4.2	18.3	1.4	27.6	3.0
Ni	9.88	3.7	16.2	1.1	25.6	6.1

[a] ASTM D 3176.
[b] Calculated according to ASTM D 3176 as 100 − C − H − N − S − ash.
[c] Determined via wet digestion with ICP.

Table 3. Distribution of C (%) among structural groups in separated swine solids ($n = 1$) and biochars at 350 and 700 °C ($n = 3$, mean and standard deviation (SD))

			350 °C biochar		700 °C biochar	
Structural group	Chemical shift (ppm)	Swine solids	Mean	SD	Mean	SD
Paraffinic	0–50	35.2	37.2	0.01	6.70	0.01
Methoxy	50–60	5.60	3.83	0.00	1.67	0.01
Alcoholic	60–96	24.4	8.93	0.00	0.60	0.00
Anomeric	96–109	6.30	3.93	0.00	4.13	0.01
Aromatic	109–145	9.80	28.6	0.01	68.2	0.02
Phenolic	145–163	4.50	7.43	0.01	3.83	0.02
Carboxylate	163–190	10.8	6.43	0.01	1.10	0.01
Carbonyl	190–220	3.50	3.57	0.01	13.70	0.01

and generated a biochar with more consistent characteristics with respect to ultimate analysis (CHNSO) coefficient of variation (CV) values. The results in Table 2 show that CV values were greater for the initial swine solids versus the 350 °C biochar. As the temperature increased to 700 °C, there were more instances of increased CV comparatively. There was a slight increase in the C content from 474 to 515 g kg_{db}^{-1} at 350 °C, followed by a decrease to 441 g kg_{db}^{-1} at 700 °C. Increasing the pyrolytic temperature decreased the HNSO composition. The mass recoveries of O and H in the 350 °C biochar were 20.4 and 50.9% respectively. With an increase in temperature, these recoveries were less than 4.5%. The H and O contents decreased owing to dehydration and degradation of C-bound O and H structures.[19] Sulfur and N were also sensitive to major vapour phase losses. Up to 53.4% of these two components were retained in the 350 °C biochar. Further heating to 700 °C caused additional releases of S and N, with N being more susceptible: 32.9 ± 0.73% of the S was recovered at 700 °C compared with only 23.1 ± 0.36% of the N. The S lost to the vapour phase during pyrolysis would have been emitted primarily as carbonyl sulfide.[18] Nitrogen losses may be due to emission of volatile organic compounds containing N.[5]

Pyrolysis concentrated plant minerals, especially P (Table 2). Total P was concentrated 57 and 138% at 350 and 700 °C respectively. When pyrolysing at 350 °C, virtually all the P (mass basis) was recovered in the biochar – 98.0 ± 2.2%; at 700 °C, however, mass recovery of P decreased to 86.9 ± 3.9%. A P recovery of 100% was reported for sewage sludge biochar processed at 450 °C.[20] The decrease in P recovery was explainable by vaporisation of P-containing compounds when temperatures approach 760 °C.[21]

The concentrations of macroelements in these manure-based biochars were greater than those for low-temperature lignocellulosic biochars. This is similar to results for pyrolysed poultry litter.[22] The concentrations of macroelements were less than those for a 450 °C sewage sludge biochar, except for Zn.[20] The concentrations for elements regulated under 40 C.F.R. § 503 (e.g. As, Cd, Cu, Mo, Ni, Zn) were lower than listed ceiling concentrations.[23] With respect to these heavy metals, this implied that swine solid biochars would not contain inorganic elements considered harmful to soils.

The ^{13}C NMR results showed that the raw feedstock was prevalent with paraffinic and alcoholic-C structures, accounting for more than 59% of the carbon distribution (Table 3). These structures were followed by approximately 10% each of aromatic and carboxylate-C structures (Table 3). The ^{13}C NMR spectral patterns show that the structural make-up of the biochars differed drastically from that of the raw feedstock owing to pyrolysis (Fig. 2 and Table 3). By increasing the pyrolytic temperature, losses occurred in the paraffinic, methoxy, alcoholic, anomeric and carboxylate-C structures. This is easily noted for the spectrum of the 700 °C biochar, which was essentially devoid of well-defined peaks characteristic of both O-containing and cellulosic compounds (e.g. peaks at 31, 57 and 75 ppm in Fig. 2). For the low-temperature biochar the paraffinic-C content averaged 37.2%, while for the 700 °C biochar it decreased to 6.7%. With these structural losses, there were increased aromatic structures, as noted by the peaks from 127 to 131 ppm (Fig. 2). The raw feedstock was characterised by 9.8% aromatic-C; aromaticity increased drastically with pyrolytic temperature to upwards of 68% (Table 3). These increases in aromaticity have also been documented in chicken litter char from fast pyrolysis at 350 °C.[24] Carbon distribution was also noted to increase for the 700 °C biochar in carbonyl-C form (peaks from 193 to 220 ppm in Fig. 2), with an average of 13.7%.

The ^{13}C NMR results suggested that these biochars were highly reproducible in structure, with standard deviations for the 350 °C biochar of less than 0.012%. Standard deviations varied more for the 700 °C biochar owing primarily to the increased ash content affecting the signal-to-noise ratio of the spectrum (Fig. 2). This was noted elsewhere for poultry litter char produced at 700 °C with an ash content of 524 g kg_{db}^{-1}.[5]

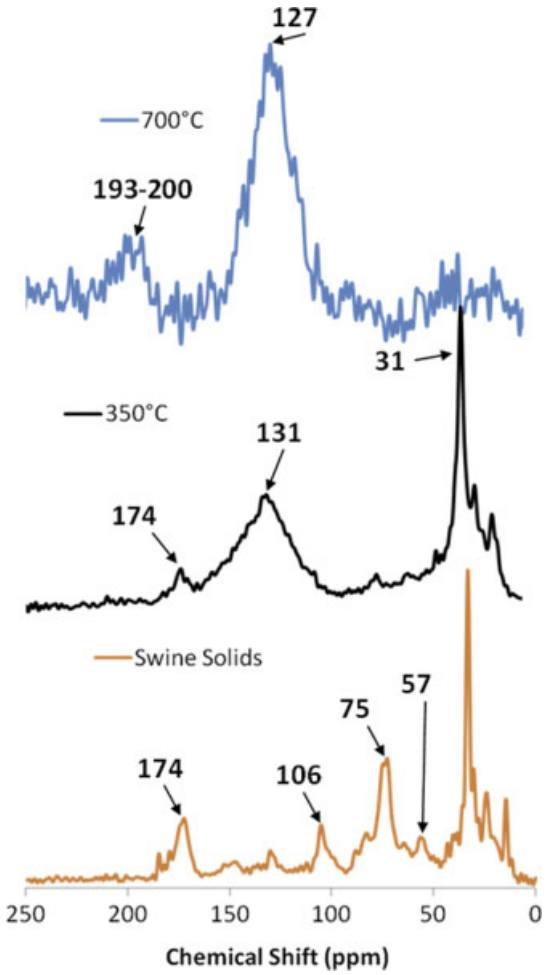

Figure 2. ^{13}C NMR spectral scans of separated swine manure solids and pyrolytic biochars at 350 and 700 °C.

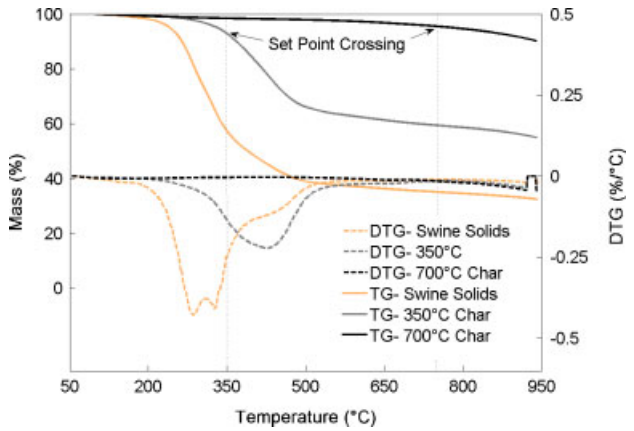

Figure 3. Mass (TG) and derivative mass (DTG) curves for swine solids, 350 °C biochar and 700 °C biochar during N_2 pyrolysis (40–950 °C, 10 °C min^{-1}). Mass (%) is the percentage ratio of actual weight to initial dry sample weight.

Biochar thermal degradation characteristics

Averaged pyrolytic and combustion mass loss (TG) and derivative of mass loss (DTG) curves for the raw feedstock and both pyrolytic temperature biochars are presented in Figs 3 and 4. The raw swine

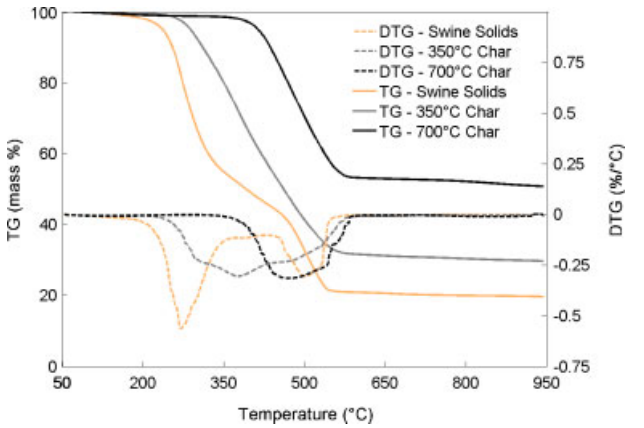

Figure 4. Mass (TG) and derivative mass (DTG) curves for swine solids, 350 °C biochar and 700 °C biochar during combustion (40–950 °C, 10 °C min^{-1}). Mass (%) is the percentage ratio of actual weight to initial dry sample weight.

solids began to devolatilise (defined here as the onset temperature for 5% conversion) at 248.7 °C, with maximum rate of mass loss (DTG) occurring at 285.0 °C (Table 4 and Fig. 3). For the 350 °C biochar, maximum DTG, which was half that of the separated swine solids, occurred at 430.4 °C. For this biochar the onset of pyrolysis did not begin until 320.5 °C. Additional pyrolysis of the 700 °C biochar exhibited no peak DTG, just a gradual mass loss of 7.2 wt%$_{db}$. In accordance with the volatile matter listed in Table 1, pyrolysis of biochars exhibited slower release of volatile matter with an increase in pyrolytic temperature: devolatilised material was greater for swine solids > 350 °C biochar > 700 °C biochar.

Combustion of the raw swine solids and associated biochars showed different characteristics than pyrolysis, demonstrating the stabilisation of the solids during the initial pyrolysis (Fig. 4). Combustion of the raw separated swine solids generated two prominent DTG peaks. Active combustion of the readily oxidised material began at 239.6 °C and peaked at 270.2 °C (Table 4); secondary combustion peaked at 501.9 °C; combustion was 90% completed at 523.0 °C. With an increase in pyrolytic temperature the two distinct combustion DTG peaks transitioned to one continuous, sustained combustion DTG peak. For the 350 °C biochar, combustion began at 289.5 °C, peaked at 377.8 °C and was 90% completed at 536.8 °C. The temperature range for combustion of the 700 °C biochar began at 410.5 °C, peaked at 469.6 °C and was 90% completed at 568.1 °C. These sustained combustion DTG peaks were attributed to the increase in fixed C (Table 1) and the increase in aromatic-C (Table 3). The combustion residual followed the same trend as the ash content in Table 1, with 700 °C > 350 °C > separated solids.

Assessing the three replicate biochars' (per temperature) profiles for both pyrolysis and combustion illustrated the high reproducibility of the controller. For both types of thermal degradation the temperatures associated with 2.5, 5, 10, 90 and 95% of total weight loss varied less than 1.7 wt%$_{db}$. This small variation across entire TG curves indicated that the biochars had near-similar structural properties, as evidenced in the ^{13}C NMR spectra, resulting in uniform degradation patterns.

CONCLUSION

High-quality designer biochar production with tailored characteristics that can target improvement of specific soil properties will

Table 4. Pyrolytic and combustion characteristics of separated swine solids and biochars at 350 and 700 °C

Process	Material	Onset temperature (°C)	Temperature at maximum rate of mass loss (°C)	Maximum rate of mass loss ($wt\%_{db}$ $°C^{-1}$)	Residual mass[a] ($wt\%_{db}$)
Pyrolysis	Swine solids	248.7	285.0	0.423	32.5
	350 °C biochar	320.5	430.4	0.213	55.0
	700 °C biochar	572.2	–	–	92.8
Combustion	Swine solids[b]	239.6	270.2	0.563	52.0
	350 °C biochar	290.4	377.8	0.306	29.7
	700 °C biochar	408.3	469.6	0.315	50.8

[a] Residual mass at end of primary reaction.
[b] Secondary combustion reaction occurred with a maximum rate of mass loss of 0.304 $wt\%_{db}$ $°C^{-1}$ at a temperature of 500.0 °C to result in a final residual mass of 19.8 $wt\%_{db}$.

require control systems that maintain pyrolytic exposure temperatures regardless of the temperature input schedule, feedstock variations or other chemical or physical anomalies within the system. Evaluation of the state-space controlled pyrolysis system at two different temperatures, 350 and 700 °C (replicates = 3), demonstrated the controller's ability to take a feedstock, in this case separated swine solids, and generate a biochar product with lower CV values with respect to ash and volatile matter contents and elemental composition (e.g. C, N, P, Zn, Mo). Further assessments of the ^{13}C NMR structure and both the pyrolytic and combustion thermal degradation patterns suggested that the biochars generated from this type of control system were highly reproducible. Thus a state-space controlled pyrolysis system would be able to generate biochars with consistent characteristics.

ACKNOWLEDGEMENTS

The authors gratefully acknowledge Dr Ray Campbell and Terra Blue, Inc. for providing swine solid samples, as well as Dr Jeff Novak for aid in editing. Mention of a trade name, proprietary product or vendor is for information only and does not guarantee or warrant the product by the USDA and does not imply its approval to the exclusion of other products or vendors that may also be suitable.

REFERENCES

1 Cantrell K, Ro K, Mahajan D, Anjom M and Hunt PG, Role of thermochemical conversion in livestock waste-to-energy treatments: obstacles and opportunities. *Ind Eng Chem Res* **46**:8918–8927 (2007).
2 Cantrell KB, Ducey T, Ro KS and Hunt PG, Livestock waste-to-bioenergy generation opportunities. *Bioresour Technol* **99**:7941–7953 (2008).
3 He BJ, Zhang Y, Funk TL, Riskowski GL and Yin Y, Thermochemical conversion of swine manure: an alternative process for waste treatment and renewable energy production. *Trans ASAE* **43**:1827–1833 (2000).
4 Florin NH, Maddocks AR, Wood S and Harris AT, High-temperature thermal destruction of poultry derived wastes for energy recovery in Australia. *Waste Manag* **29**:1399–1408 (2009).
5 Novak JM, Lima I, Baoshan X, Gaskin JW, Steiner C, Das KC, *et al*, Characterization of designer biochar produced at different temperatures and their effects on a loamy sand. *Ann Environ Sci* **3**:195–206 (2009).
6 Glaser B, Lehmann J and Zech W, Ameliorating physical and chemical properties of highly weathered soils in the tropics with charcoal – a review. *Biol Fertil Soils* **35**:219–230 (2002).
7 Novak JM, Busscher WJ, Laird DL, Ahmedna M, Watts DW and Niandou MAS, Impact of biochar amendment on fertility of a southeastern coastal plain soil. *Soil Sci* **174**:105–112 (2009).
8 Chan KY and Xu Z, Biochar: nutrient properties and their enhancement, in *Biochar for Environmental Management: Science and Technology*, ed. by Lehmann J and Joseph S. Earthscan, Sterling, VA, pp. 67–84 (2009).
9 Roberts KG, Gloy BA, Joseph S, Scott NR and Lehmann J, Life cycle assessment of biochar systems: estimating the energetic, economic, and climate change potential. *Environ Sci Technol* **44**:827–833 (2010).
10 Mulvaney SJ, Rizvi SSH and Johnson JCR, Dynamic modeling and computer control of a retort for thermal processing. *J Food Eng* **11**:273–289 (1990).
11 Alonso AA, Banga JR and Perez-Martin R, A complete dynamic model for the thermal processing of bioproducts in batch units and its application to controller design. *Chem Eng Sci* **52**:1307–1322 (1997).
12 Alonso AA, Banga JR and Perez-Martin R, Modeling and adaptive control for batch sterilization. *Comput Chem Eng* **22**:445–458 (1998).
13 Cantrell KB and Martin II JH, Stochastic state-space temperature regulation of biochar production. Part I: Theoretical development. *J Sci Food Agric* **00**:000–000 (2011).
14 Vanotti MB, Szogi AA, Millner PD and Loughrin JH, Development of a second-generation environmentally superior technology for treatment of swine manure in the USA. *Bioresour Technol* **100**:5406–5416 (2009).
15 ASTM, *Petroleum Products, Lubricants, and Fossil Fuels: Gaseous Fuels, Coal, and Coke*. ASTM International, West Conshohocken, PA (2006).
16 Cantrell KB, Martin II JH and Ro KS, Application of thermogravimetric analysis for the proximate analysis of livestock wastes. *J ASTM Int* **7**:Paper ID JAI102583 (2010).
17 Ghosh S, Wang ZY, Kang S, Bhowmik PC and Xing BS, Sorption and fractionation of a peat derived humic acid by kaolinite, montmorillonite, and goethite. *Pedosphere* **19**:21–30 (2009).
18 Ro KS, Cantrell KB and Hunt PG, High-temperature pyrolysis of blended animal manures for producing renewable energy and value-added biochar. *Ind Eng Chem Res* **49**:10125–10131 (2010).
19 Antal Jr MJ and Grønli M, The art, science, and technology of charcoal production. *Ind Eng Chem Res* **42**:1619–1640 (2003).
20 Bridle TR and Pritchard D, Energy and nutrient recovery from sewage sludge via pyrolysis. *Water Sci Technol* **50**:169–175 (2004).
21 Knicker H, How does fire affect the nature and stability of soil organic nitrogen and carbon? A review. *Biogeochemistry* **85**:91–118 (2007).
22 Gaskin JW, Steiner C, Harris K, Das KC and Bibens B, Effect of low-temperature pyrolysis conditions on biochar for agricultural use. *Trans ASABE* **51**:2061–2069 (2008).
23 US EPA, *Protection of Environment. Standards for the Use or Disposal of Sewage Sludge. Code of Federal Regulations. Title 40, Pt. 503*. US Environmental Protection Agency, Washington, DC (2005).
24 Schnitzer MI, Monreal CM, Facey GA and Fransham PB, The conversion of chicken manure to biooil by fast pyrolysis. I. Analyses of chicken manure, biooils and char by ^{13}C and ^{1}H NMR and FTIR spectrophotometry. *J Environ Sci Health B* **42**:71–77 (2007).